Pediatric RESEARCH

BASIC SCIENCE ARTICLE

Troponin T amino acid mutation (ΔK210) knock-in mice as a neonatal dilated cardiomyopathy model

Jun Tanihata[1], Teruyuki Fujii[1,2], Shunsuke Baba[1], Yoshitaka Fujimoto[1,3], Sachio Morimoto[4] and Susumu Minamisawa[1]

BACKGROUND: Dilated cardiomyopathy (DCM) in children is often associated with poor morbidity and mortality and exhibits distinct pathological entities from those of adult DCM. Owing to the limited number of patients and the lack of a good animal model, the molecular mechanisms underlying pediatric DCM remain poorly understood. The purpose of this study is to establish an animal model of neonatal DCM and identify early progression factors.
METHODS: Cardiac phenotypes and comprehensive gene expression profiles in homozygous ΔK210 knock-in (*TNNT2*$^{\Delta K210/\Delta K210}$) mice were analyzed and compared to *TNNT2*$^{+/\Delta K210}$ and wild-type mice at 0 days and 1 week of age.
RESULTS: Immediately after birth, the cardiac weight in *TNNT2*$^{\Delta K210/\Delta K210}$ mice was already increased compared to that in *TNNT2*$^{+/\Delta K210}$ and wild-type mice. Echocardiographic examination of 0-day-old and 1-week-old *TNNT2*$^{\Delta K210/\Delta K210}$ mice revealed similar phenotypes of pediatric DCM. In addition, several genes were significantly upregulated in the ventricular tissues of *TNNT2*$^{\Delta K210/\Delta K210}$ mice, and the KEGG PATHWAY analysis revealed several important pathways such as cancer and focal adhesion that might be associated with the pathogenesis and development of DCM.
CONCLUSIONS: *TNNT2*$^{\Delta K210/\Delta K210}$ mice have already developed DCM at birth, indicating that they should be an excellent animal model to identify early progression factors of DCM.

Pediatric Research (2021) 89:846–857; https://doi.org/10.1038/s41390-020-1016-1

IMPACT:

- *TNNT2*$^{\Delta K210/\Delta K210}$ mice are excellent animal model for DCM.
- *TNNT2*$^{\Delta K210/\Delta K210}$ mice are excellent animal model to identify early progression factors of DCM.
- KEGG PATHWAY analysis revealed that several important pathways such as cancer and focal adhesion might be associated with the pathogenesis and development of neonatal DCM.

INTRODUCTION

Dilated cardiomyopathy (DCM) is characterized by cardiac dilation and pump failure. It is the most common type of cardiomyopathy and heart failure in children and is diagnosed in 0.57 of every 100,000 children per year in the United States.[1,2] Among DCM patients who are diagnosed at or before 10 years of age, 20% are diagnosed during the neonatal period (<4 weeks old) and another 65% are diagnosed in the first year of life.[3] Approximately half of all children with DCM either die or undergo heart transplantation within the first 5 years.[2] In 20–45% of pediatric patients with DCM, on the other hand, cardiac function can be normalized.[4] Recent studies have indicated that pediatric and adult DCM are distinct pathological entities.[5,6] For example, the gene profiles and responses to stress in pediatric DCM are different from those in adult DCM.[4] Despite tremendous efforts to improve available treatment protocols, outcomes of children with DCM have improved little and heart transplantation is almost the only therapeutic strategy. The reasons for our lack of progress in this regard include the limited number of patients and the lack of a good animal model for pediatric DCM. A useful animal model is therefore highly desirable as it will enable us to more thoroughly investigate the molecular mechanisms underlying pediatric DCM.

Of the DCM patients who are diagnosed at or before 10 years of age, 15% are considered to have familial DCM.[3] Pediatric DCM is often associated with mutations in sarcomeric and cytoskeletal genes. Cardiac troponin T (*TNNT2*) exon 13 lysine deletions (ΔK210) often result in a rapid progression of heart failure or sudden cardiac death at a young age.[7–9] To clarify the causal mechanisms of DCM, *TNNT2* ΔK210 knock-in mice have been generated; these exhibit phenotypes similar to those in human DCM, including premature death.[10] Homozygous or heterozygous ΔK210 knock-in (*TNNT2*$^{\Delta K210/\Delta K210}$ or *TNNT2*$^{+/\Delta K210}$) mice start to die at approximately 10 or 30 days after birth, respectively.[10] Only 20% of *TNNT2*$^{\Delta K210/\Delta K210}$ mice can survive longer than 4 months. Therefore, ΔK210 knock-in mice are considered to be an excellent animal model of pediatric DCM. In spite of their usefulness, however, the phenotypes of ΔK210 knock-in mice have not been extensively analyzed during the neonatal and weaning periods. The purpose of the present study is to investigate these early phenotypes of *TNNT2*$^{\Delta K210/\Delta K210}$ mice from birth and to explore

[1]Department of Cell Physiology, The Jikei University School of Medicine, Tokyo, Japan; [2]Department of Anesthesiology, The Jikei University Kashiwa Hospital, Chiba, Japan; [3]Department of Pediatrics, Gyoda General Hospital, Saitama, Japan and [4]School of Health Science, International University of Health and Welfare, Fukuoka, Japan
Correspondence: Susumu Minamisawa (sminamis@jikei.ac.jp)

Received: 18 September 2019 Revised: 25 April 2020 Accepted: 1 June 2020
Published online: 20 June 2020

the molecular mechanisms underlying the poor prognosis of *TNNT2*$^{\Delta K210/\Delta K210}$ mice.

MATERIALS AND METHODS

Animals

Wild-type, *TNNT2*$^{+/\Delta K210}$, and *TNNT2*$^{\Delta K210/\Delta K210}$ mice were used throughout this study and were examined either immediately after birth (0 days old) or 1 week after birth (1 week old). To obtain tissue samples, all animals were anesthetized with isoflurane, and cervical dislocation was performed after loss of pain reflex. Thereafter, the heart was immediately excised and weighed. A portion of each animal's ventricular tissues was frozen in liquid nitrogen as a sample for gene expression analysis and another portion was soaked in 10% formaldehyde neutral buffer solution (Nacalai Tesque, Inc., Kyoto, Japan) for histological examination. The animal experiments were performed in accordance with the NIH guidelines (Guide for the Care and Use of Laboratory Animals). All animal studies were approved by the Institutional Animal Care and Use Committee of The Jikei University.

Echocardiography

To evaluate the global morphology and function of the heart, echocardiography was performed at 0 days and 1 week of age in three groups of mice. All mice were sedated with 1.5% isoflurane using an up to 70-MHz transducer from the Vevo 3100 Imaging System (FUJIFILM VisualSonic Inc., Toronto, Canada). Measurements were performed using the analysis software Vevo LAB (FUJIFILM VisualSonic Inc.). Interventricular septum (IVS), left ventricular (LV) diameter at end diastole, LV diameter at end systole, posterior LV wall thickness (PWT), ejection fraction (EF), and LV end-diastolic volume were measured at the papillary muscle level of the LV using a short-axis view.

Histological examination

The excised ventricular tissues of wild-type, *TNNT2*$^{+/\Delta K210}$, and *TNNT2*$^{\Delta K210/\Delta K210}$ mice at 0 days and 1 week of age were subjected to hematoxylin–eosin (HE) and Masson trichrome staining. Each sample was observed under a light microscope at 10 times magnification. The photographed images were converted to combined images using BZ-9000 (KEYENCE, Osaka, Japan) to estimate the fibrosis area in Masson trichrome staining as previously described.[11]

DNA microarray analysis

Total RNAs were extracted from ventricular tissue in wild-type and *TNNT2*$^{\Delta K210/\Delta K210}$ mice at 0 days and 1 week of age using TRIZOL reagent (Thermo Fisher Scientific, Waltham, MA, USA). Three ventricular samples from each group were combined for comparison. RNA purity and integrity were evaluated using an ND-1000 Spectrophotometer (NanoDrop, Wilmington, DE, USA) and an Agilent 2100 Bioanalyzer (Agilent Technologies, Palo Alto, CA, USA). Total RNA labeling and hybridization were performed using the Agilent One-Color Microarray-Based Gene Expression Analysis protocol (Agilent Technologies, V 6.5, 2010). Briefly, 100 ng of total RNA was labeled with Cy3-dCTP. The labeled cRNAs were purified using an RNAeasy Mini Kit (Qiagen, Hilden, Germany). The concentration and specific activity of the labeled cRNAs (pmol Cy3/μg cRNA) were measured using the NanoDrop ND-1000 Spectrophotometer. Hybridization was performed according to the supplier's instructions (Agilent Technologies, V 6.5, 2010). Six hundred nanograms of each labeled cRNA was fragmented by adding 5 μl 10× blocking agent and 1 μl of 25× fragmentation buffer, and then heated at 60 °C for 30 min. Finally, 25 μl 2× GE hybridization buffer was added to dilute the labeled cRNA. Forty microliters of hybridization solution was dispensed into the gasket slide and assembled to the Agilent SurePrint G3 Mouse GE 8 × 60K Microarrays (Agilent). The slides were incubated for 17 h at 65 °C in an Agilent hybridization oven and then washed at room temperature according to the Agilent One-Color Microarray-Based Gene Expression Analysis protocol (Agilent Technologies, V 6.5, 2010). Hybridization signals were immediately scanned with an Agilent Microarray Scanner D (Agilent Technologies). Microarray results were extracted using the Agilent Feature Extraction software v11.0 (Agilent Technologies). Array probes that had Flag A in their samples were filtered out. Selected gProcessedSignal value was transformed by logarithm and normalized according to the quantile method. Statistical significance of the expression data was determined using local pooled error test and fold change in which the null hypothesis was that no difference exists among groups. False discovery rate was controlled by adjusting the *p* value by means of the Benjamini–Hochberg algorithm. For a differentially expressed gene set, hierarchical cluster analysis was performed using complete linkage and Euclidean distance as a measure of similarity. Gene Enrichment and Functional Annotation analysis for significant probe list was performed using the Kyoto Encyclopedia of Genes and Genomes (KEGG) PATHWAY database (www.genome.jp/kegg/).[12] All data analysis and visualization of DEGs was conducted using R 3.1.2 (www.r-project.org). The complete data set of the DNA microarray is available in the Gene Expression Omnibus database (accession number: GSE133052).

Real-time PCR analysis

Extraction of total RNA from ventricular tissues from wild-type, *TNNT2*$^{+/\Delta K210}$, and *TNNT2*$^{\Delta K210/\Delta K210}$ mice at 0 days and 1 week of age, generation of cDNA, and reverse transcription PCR (RT-PCR) analysis were performed as described previously.[11] Natriuretic peptide type A (ANF), brain natriuretic factor (BNF), connective tissue growth factors (CTGFs), glial cell line-derived neurotrophic factor (Gdnf), secreted phosphoprotein 1 (Spp1), protein phosphatase 1, regulatory (inhibitor) subunit 12B (Ppp1r12b), sarcolipin (SLN), phospholamban (PLN), calsequestrin 1 (CSQ1) and 2 (CSQ2), sarcoplasmic reticulum (SR)/endoplasmic reticulum Ca^{2+}-ATPase 2a (SERCA2a), ryanodine receptor type 2 (RyR2) troponin T type A (TnT A) and E (TnT E), cardiac troponin I (cTnI), slow skeletal type troponin I (ssTnI), cardiac troponin C (cTnC), and cardiac tropomyosin (cTM) expression levels in the ventricular tissues were measured in the wild-type, *TNNT2*$^{+/\Delta K210}$, and *TNNT2*$^{\Delta K210/\Delta K210}$ mice at 0 days and 1 week of age using real-time PCR. The primer nucleotide sequences are shown in Supplementary Table S1. Glyceraldehyde 3-phosphate dehydrogenase (GAPDH) expression level was quantitated as an internal control.

Western blot analysis

Protein was extracted from ventricular tissues from wild-type and *TNNT2*$^{\Delta K210/\Delta K210}$ mice at 0 days and 1 week of age. Ventricular tissues were lysed in RIPA buffer containing phenylmethylsulfonyl fluoride, protease inhibitor, and sodium orthovanadate (Santa Cruz Biotechnology, CA, USA). Samples were centrifuges at 15,000 rpm for 10 min, and the protein concentration of supernatants was determined using the BCA Protein Assay Kit (TAKARA Bio Inc., Shiga, Japan). An aliquot of the extracted protein solution was mixed with sample buffer solution (Nacalai Tesque, Inc., Kyoto, Japan), and the mixture was heated at 95 °C for 5 min. Thirty micrograms of protein were separated on 4–20% gradient sodium dodecyl sulfate polyacrylamide gel electrophoresis (SDS PAGE) gels (Bio-Rad, CA, USA) and electrically transferred from the gels to a polyvinylidene difluoride membrane (Merck Millipore, MA, USA). After blocking with 5% skim milk in TBS with 0.05% Tween-20,

Table 1. Neonatal *TNNT2*$^{\Delta K210/\Delta K210}$ mice displayed a significant increase in heart/body weight ratio.

	At birth			3–4 days			1 week		
	WT	+/ΔK210	ΔK210/ΔK210	WT	+/ΔK210	ΔK210/ΔK210	WT	+/ΔK210	ΔK210/ΔK210
n	22	31	14	10	17	10	14	21	10
BW (g)	1.52 ± 0.04	1.37 ± 0.03	1.38 ± 0.03	2.42 ± 0.18	2.56 ± 0.10	2.50 ± 0.15	5.00 ± 0.20	4.67 ± 0.16	4.82 ± 0.19
HW (mg)	8.74 ± 0.25**	8.34 ± 0.19**	11.45 ± 0.27	12.78 ± 1.23*	13.24 ± 0.68**	17.4 ± 1.95	28.31 ± 0.91**	29.61 ± 1.06**	38.17 ± 2.47
HW/BW (mg/g)	5.83 ± 0.17**	6.09 ± 0.11**	8.31 ± 0.15	5.23 ± 0.16**	5.17 ± 0.16**	6.85 ± 0.35	5.71 ± 0.14**	6.39 ± 0.19**	7.93 ± 0.40

Data represent the mean ± SE. Statistical analysis was determined by ANOVA followed by post hoc Tukey's multiple comparison test.
WT wild type, *BW* body weight, *HW* heart weight, *HW/BW* heart weight-to-body weight ratio.
*$p < 0.05$ and **$p < 0.01$ vs age-matched wild-type.

primary antibodies were applied to the membrane overnight at 4 °C. After washing, the membranes were incubated with horseradish peroxidase-conjugated secondary antibody. The signals were detected using the West Dura Extended Duration Substrate (Thermo Fisher Scientific, MA, USA). The band intensities of the target proteins were analyzed using the NIH Image J software and normalized by the band intensity of GAPDH (Cell Signaling Technology, MA, USA). The primary antibodies used in this study were as follows: anti-col4a5 (Genetex, CA, USA), anti-Birc5 (Cell Signaling Technology, MA, USA), anti-Lpar3 (Abcam, Tokyo, Japan), anti-Fos (Cell Signaling Technology, MA, USA), anti-troponin I (Cell Signaling Technology, MA, USA), anti-phospho-troponin I (Ser23/34) (Cell Signaling Technology, MA, USA), and anti-GAPDH (Cell Signaling Technology, MA, USA). For sarcomeric protein detection, 10 μg of protein were separated on 10% SDS PAGE gels (Bio-Rad, CA, USA) and the SYPRO Ruby Protein Gel Stain (Thermo Fisher Scientific, MA, USA) was used according to the manufacturer's protocol.

Statistical analysis

Results are presented as the mean ± standard error of the mean (SEM). Surgical and echocardiographic findings and various mRNA expression levels from real-time PCR were compared between these groups using analysis of variance followed by post hoc Tukey's multiple comparison test. $p < 0.05$ was considered significant.

RESULTS

Neonatal *TNNT2*$^{\Delta K210/\Delta K210}$ mice displayed a dilated cardiomyopathic phenotype

Neonatal *TNNT2*$^{\Delta K210/\Delta K210}$ mice displayed a significant increase in heart/body weight ratio when compared with wild-type mice and *TNNT2*$^{+/\Delta K210}$ mice at 0 days of age (Table 1), whereas the heart/body weight ratio was not different between wild-type mice and *TNNT2*$^{+/\Delta K210}$ mice at either 0 days or 1 week of age. At neither age was there any significant difference in body weight among the three groups. After Masson trichrome staining, representative horizontal sections of the heart at the papillary muscle level are shown in Fig. 1a. There was no difference in the incidence or distribution of fibrotic areas and disarray of cardiomyocytes among the three groups at birth or 1 week after birth (Fig. 1b), although previous studies have reported that marked interstitial fibrosis developed in the ventricles of 6-week-old *TNNT2*$^{\Delta K210/\Delta K210}$ mice.[10] After HE staining, myofibril organization also remained normal in *TNNT2*$^{+/\Delta K210}$ and *TNNT2*$^{\Delta K210/\Delta K210}$ mice at birth and 1 week after birth (Supplementary Fig. S1). Echocardiographic examination of 0-day-old neonatal mice revealed that no significant difference in LV EF (Fig. 2f), an index of systolic function, among the three groups, whereas LV end-diastolic dimension (Fig. 2c) and volume (Fig. 2e) were significantly increased in *TNNT2*$^{\Delta K210/\Delta K210}$ mice as compared with wild-type

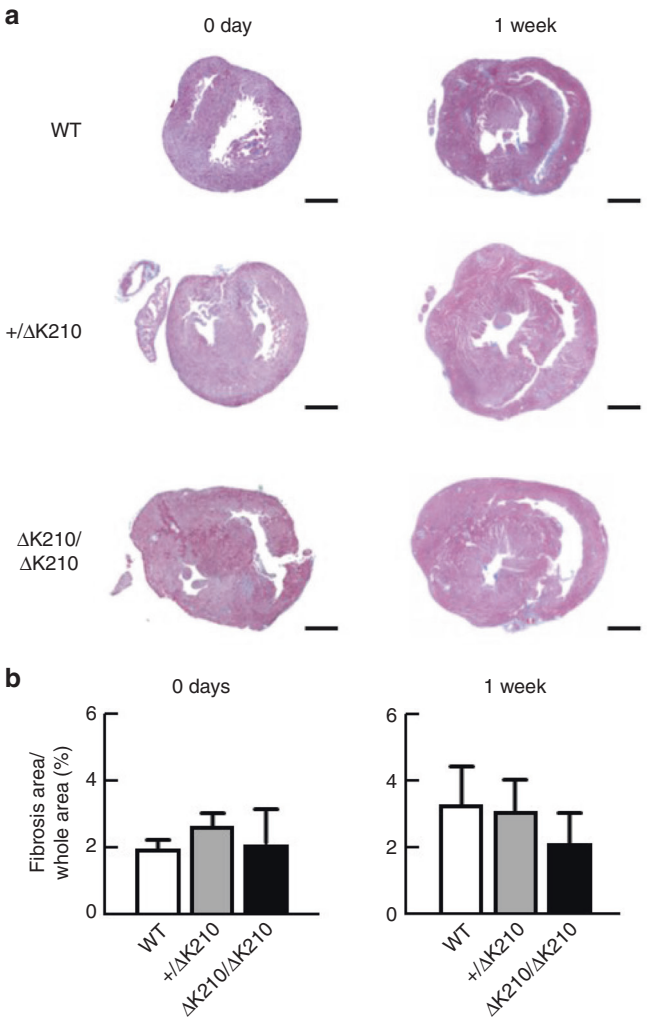

Fig. 1 No extensive fibrosis in the hearts of neonatal *TNNT2*$^{\Delta K210/\Delta K210}$ mice. a Representative histological sections were stained with Masson trichrome staining in the heart at the papillary muscle level of WT, *TNNT2*$^{+/\Delta K210}$, and *TNNT2*$^{\Delta K210/\Delta K210}$ mice at 0 days and 1 week of age. Scale bars are 500 μm. **b** Quantification of fibrotic areas in the hearts of WT ($n = 7$), *TNNT2*$^{+/\Delta K210}$ ($n = 8$) and *TNNT2*$^{\Delta K210/\Delta K210}$ ($n = 5$) mice at 0 days and 1 week of age. Data are shown as mean ± SEM.

mice. Echocardiographic examination of 1-week-old neonatal mice also revealed that LV end-diastolic dimension (Fig. 2c) and volume (Fig. 2e) were significantly increased in *TNNT2*$^{\Delta K210/\Delta K210}$ mice as compared with wild-type and *TNNT2*$^{+/\Delta K210}$ mice, and that

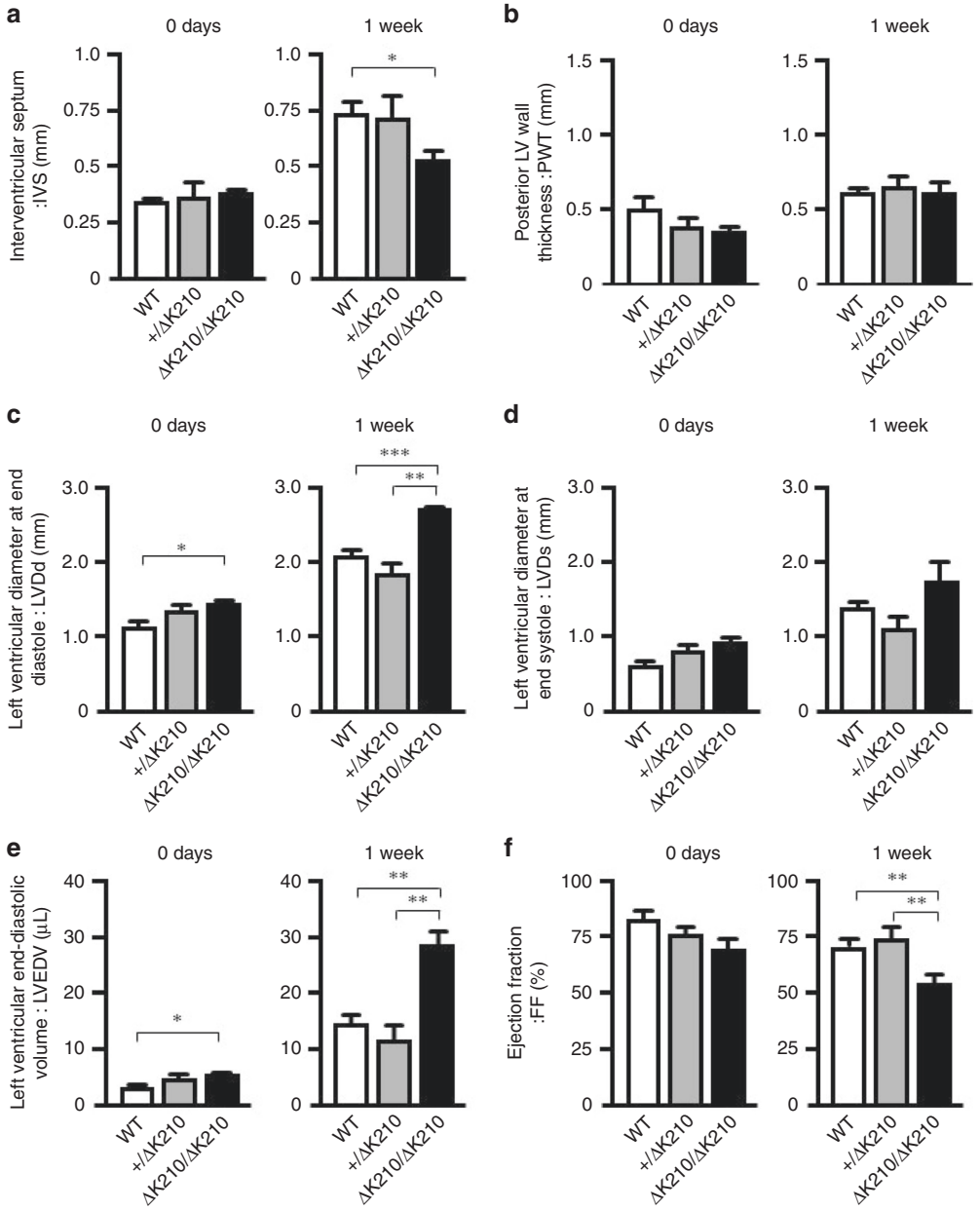

Fig. 2 Reduction of cardiac systolic function in 0-day-old and 1-week-old neonatal *TNNT2*$^{\Delta K210/\Delta K210}$ mice. Echocardiographic examination of 0-day-old ($n = 3$–4 per group) and 1-week-old ($n = 5$–6 per group) neonatal WT, *TNNT2*$^{+/\Delta K210}$, and *TNNT2*$^{\Delta K210/\Delta K210}$ mice. **a** Interventricular septal (IVS) thickness, **b** posterior left ventricular wall thickness (PWT), **c** left ventricular diameter at end diastole (LVDd), **d** left ventricular diameter at end systole (LVDs), **e** left ventricular end-diastolic volume (LVEDV), and **f** ejection fraction. Data are shown as mean ± SEM. *$p < 0.05$, **$p < 0.01$, ***$p < 0.001$ by ANOVA followed by post hoc Tukey's multiple comparison test.

LV EF (Fig. 2f) was significantly reduced in *TNNT2*$^{\Delta K210/\Delta K210}$ mice as compared with wild-type and *TNNT2*$^{+/\Delta K210}$ mice. IVS thickness (Fig. 2a) was significantly thinner in 1-week-old *TNNT2*$^{\Delta K210/\Delta K210}$ mice than in wild-type and *TNNT2*$^{+/\Delta K210}$ mice, whereas no significant differences were detected in LV PWT among the three groups at either 0 days or 1 week of age (Fig. 2b).

DNA microarray analyses revealed distinct transcriptional profiles of *TNNT2*$^{\Delta K210/\Delta K210}$ mice

We performed microarray analysis with pooled LV tissues from wild-type and *TNNT2*$^{\Delta K210/\Delta K210}$ mice at 0 days ($n = 2$ for each genotype) and 1 week of age ($n = 2$ for each genotype). The degree of similarity in the transcriptional profiles between the wild-type and *TNNT2*$^{\Delta K210/\Delta K210}$ mice was calculated, and the profiles of gene expression were grouped into two distinct clusters: a 0-day-old cluster and a 1-week-old cluster (Supplementary Fig. S2), suggesting that the effect of development on the gene profiles is much greater than the effect of genotype. Nevertheless, we found that 12 gene probes at 0 days of age (Table 2) and 53 gene probes at 1 week of age (Table 3) were significantly upregulated (fold change = ≥2.0 and p value < 0.05) in the pooled ventricular tissues of *TNNT2*$^{\Delta K210/\Delta K210}$ mice as compared with those of wild-type mice. Two genes (calsequestrin 1 and contactin 2) were significantly upregulated in *TNNT2*$^{\Delta K210/\Delta K210}$ mice of both ages. On the other hand, we found that 20 gene probes at 0 days of age (Table 4) and 30 gene probes at 1 week of age (Table 5) were

Table 2. Twelve gene probes at 0 days of age were significantly upregulated in the pooled ventricular tissues of *TNNT2*$^{\Delta K210/\Delta K210}$ mice.

Upregulated at birth					
	Gene_Symbol	Gene name	Fold change	Probe ID	Genbank accession
1	Gm11783	Predicted gene 11783	29.28	A_55_P2256586	XR_406739
2	Cradd	CASP2 and RIPK1 domain containing adaptor with death domain	6.51	A_55_P2177386	NM_009950
3	Rnu3b1	U3B small nuclear RNA 1	4.83	A_55_P2009217	NR_004415
4	Sorbs2	Sorbin and SH3 domain containing 2	4.36	A_51_P368139	AK049030
5			3.37	A_66_P109246	CA584427
6	Rs5-8s1	5.8S ribosomal RNA	3.32	A_55_P1977776	NR_003280
7	Vwc2	von Willebrand factor C domain containing 2	3.04	A_55_P2903049	NM_177033
8	Cntn2	Contactin 2	2.98	A_52_P628702	NM_177129
9	Gzma	Granzyme A	2.56	A_55_P2094060	NM_010370
10	Nav2	Neuron navigator 2	2.50	A_55_P2714682	AK162444
11	Casq1	Calsequestrin 1	2.40	A_55_P2856642	NM_009813
12	Xlr4b	X-linked lymphocyte-regulated 4B	2.00	A_51_P457244	NM_021365

significantly downregulated (fold change = ≤−2.0 and p value < 0.05) in the pooled ventricular tissues of *TNNT2*$^{\Delta K210/\Delta K210}$ mice as compared with those of wild-type mice. Three genes (secreted phosphoprotein 1, Rab7b, and AK041267) were significantly downregulated in *TNNT2*$^{\Delta K210/\Delta K210}$ mice of both ages.

To analyze the interaction networks and reaction networks of the genes that have distinct expression levels in *TNNT2*$^{\Delta K210/\Delta K210}$ mice as compared to wild-type mice, we performed the KEGG PATHWAY analysis using the KEGG database.[12] There was significant ($p < 0.05$) overrepresentation of genes involved in five KEGG pathways in *TNNT2*$^{\Delta K210/\Delta K210}$ mice as compared with wild-type mice and *TNNT2*$^{\Delta K210/\Delta K210}$ mice at 1 week of age, namely, cancer, focal adhesion, cardiac muscle contraction, adrenergic signaling in cardiomyocytes, and phosphatidylinositol 3-kinase-Akt signaling pathways (Fig. 3).

RT-PCR analysis verified the expression patterns of DNA microarray analyses of *TNNT2*$^{\Delta K210/\Delta K210}$ mice

To verify the results of the microarray, we performed quantitative RT-PCR for ANF, BNF, CTGF, Gdnf, Spp1, and Ppp1r12b. We found that ANF levels was highly expressed in the ventricles of 1-week-old *TNNT2*$^{\Delta K210/\Delta K210}$ mice compared to wild-type and *TNNT2*$^{+/\Delta K210}$ mice; at birth, in contrast, the expression levels of ANF mRNA were not different among the three groups (Fig. 4a). The expression levels of BNF (Fig. 4b) and CTGF (Fig. 4c), on the other hand, were not different among the three groups at either 0 days or 1 week of age. Furthermore, we found that the expression levels of Gdnf were significantly higher in *TNNT2*$^{\Delta K210/\Delta K210}$ mice than in wild-type mice at both 0 days and 1 week (Fig. 4d). The expression levels of Spp1 (Fig. 4e) and Ppp1r12b (Fig. 4f) were significantly lower in *TNNT2*$^{\Delta K210/\Delta K210}$ mice than in wild-type mice at 0 days; at 1 week of age, Spp1 levels remained significantly lower in *TNNT2*$^{\Delta K210/\Delta K210}$ mice, while Ppp1r12b levels were comparable between *TNNT2*$^{\Delta K210/\Delta K210}$ and wild-type mice. These data supported our DNA microarray results.

Western blot analysis verified the expression patterns of DNA microarray analysis of *TNNT2*$^{\Delta K210/\Delta K210}$ mice

To determine whether TNNT2 K210 deletion induces alterations in the expression levels of other sarcomeric proteins, we investigated total protein using SYPRO Ruby Protein Gel Stain. Sarcomeric protein expression levels were not significantly different between wild-type and *TNNT2*$^{\Delta K210/\Delta K210}$ mice at either 0 days or 1 week of age (Supplementary Fig. S3). To verify the results of the DNA microarray analysis, we performed western blot analysis for Col4a5, Birc5, Lpar3, and Fos. The protein expression level of Birc5 was higher in *TNNT2*$^{\Delta K210/\Delta K210}$ mice than in wild-type mice, while Col4a5, Lpar3, and Fos expression levels were comparable between *TNNT2*$^{\Delta K210/\Delta K210}$ and wild-type mice at 0 days of age (Fig. 5a). The protein expression levels of Col4a5, Lpar3, and Birc5 were found to be upregulated, and Fos expression levels were found to be downregulated in *TNNT2*$^{\Delta K210/\Delta K210}$ mice as compared to wild-type mice at 1 week of age (Fig. 5b, c). These results are consistent with the results of DNA microarray analysis shown in Tables 3 and 5.

The changes in transcription profiles of SR-related genes in *TNNT2*$^{\Delta K210/\Delta K210}$ mice

Next, we examined the expression levels of genes related to the SR because SR dysfunction is known to be one of the earliest insults in heart failure. We found that SLN (Supplementary Fig. S4A) and CSQ1 (Supplementary Fig. S4C) were significantly upregulated in *TNNT2*$^{\Delta K210/\Delta K210}$ mice at 1 week of age, which is consistent with our DNA microarray data. In addition, the expression levels of CSQ2 were significantly increased in *TNNT2*$^{\Delta K210/\Delta K210}$ mice at 1 week of age compared to those in wild-type and *TNNT2*$^{+/\Delta K210}$ mice (Supplementary Fig. S4D). With regard to PLN (Supplementary Fig. S4B), SERCA2a (Supplementary Fig. S4E), and RyR2 (Supplementary Fig. S4F) mRNAs, in contrast, there was no difference among the three groups at either 0 days or 1 week of age.

The changes in transcription profiles of troponin-related genes in *TNNT2*$^{\Delta K210/\Delta K210}$ mice

We also investigated whether troponin T amino acid mutation (ΔK210) may change the composition of troponin T isoforms and troponin T-related myofibril proteins in *TNNT2*$^{\Delta K210/\Delta K210}$ mice during the early neonatal period. Our examination of the expression levels of isoforms of troponin T (A-type: fatal form or E-type: adult form), isoforms of troponin I (cardiac type or slow skeletal type), cardiac/slow skeletal troponin C, and tropomyosin 1 revealed no significant differences among the three groups (Fig. 6). To verify the effects of troponin mutation on sarcomere protein phosphorylation, we examined the phosphorylation levels of

Table 3. Fifty-three gene probes at 1 week of age were significantly upregulated in the pooled ventricular tissues of *TNNT2*$^{\Delta K210/\Delta K210}$ mice.

Upregulated at 1 week					
	Gene_Symbol	Gene name	Fold change	Probe ID	Genbank accession
1	Casq1	Calsequestrin 1	6.55	A_55_P2856642	NM_009813
2	Myh7	Myosin, heavy polypeptide 7, cardiac muscle, beta	5.95	A_55_P2093232	NM_080728
3	Acsl3	Acyl-CoA synthetase long-chain family member 3	3.65	A_55_P2165324	NM_028817
4	Col4a5	Collagen, type IV, alpha 5	3.65	A_51_P216005	NM_007736
5	Sln	Sarcolipin	3.61	A_52_P413395	NM_025540
6	Proser1	Proline and serine rich 1	3.59	A_52_P258218	NM_173382
7	Cdh3	Cadherin 3	3.54	A_66_P113868	NM_001037809
8	Commd6	COMM domain containing 6	3.45	A_52_P446120	NM_001033132
9	Nppa	Natriuretic peptide type A	3.45	A_55_P2745418	NM_008725
10	Gdnf	Glial cell line-derived neurotrophic factor	3.28	A_55_P2045896	NM_010275
11	Fmnl2	Formin-like 2	2.99	A_52_P640296	NM_172409
12	Nppa	Natriuretic peptide type A	2.94	A_52_P580582	NM_008725
13	4833412C05Rik	RIKEN cDNA 4833412C05 gene	2.92	A_66_P105418	NR_045954
14	Cntn2	Contactin 2	2.91	A_52_P628702	NM_177129
15	Myl7	Myosin, light polypeptide 7, regulatory	2.86	A_51_P246345	NM_022879
16	Xlr4b	X-linked lymphocyte-regulated 4B	2.8	A_55_P2046101	NM_021365
17	Xlr4a	X-linked lymphocyte-regulated 4A	2.76	A_55_P2124586	NM_001081642
18			2.71	A_52_P210270	AK089956
19	Gm1043	Predicted gene 1043	2.71	A_55_P2723949	XM_011251988
20	Sphkap	SPHK1 interactor, AKAP domain containing	2.69	A_55_P2033849	NM_172430
21			2.66	A_66_P113438	ENSMUST00000181879
22	Hist2h3c2	Histone cluster 2, H3c2	2.65	A_66_P127991	BC015270
23			2.65	A_30_P01020675	chr16:23534663-23535172_F
24			2.53	A_51_P201445	ENSMUST00000120976
25	Scgb3a2	Secretoglobin, family 3A, member 2	2.52	A_51_P303097	NM_001289643
26	Nmrk2	Nicotinamide riboside kinase 2	2.52	A_51_P369762	NM_027120
27	Sphkap	SPHK1 interactor, AKAP domain containing	2.48	A_66_P107886	ENSMUST00000160953
28	Spc25	SPC25, NDC80 kinetochore complex component, homolog (*S. cerevisiae*)	2.46	A_51_P514700	NM_025565
29	Lman1l	Lectin, mannose-binding 1 like	2.45	A_51_P367263	NM_199222
30	LOC105245882	Transcription factor BTF3 pseudogene	2.45	A_55_P2022699	XR_875022
31	Stam2	Signal transducing adaptor molecule (SH3 domain and ITAM motif) 2	2.42	A_55_P2174339	ENSMUST00000155516
32	Hey2	Hairy/enhancer-of-split related with YRPW motif 2	2.41	A_51_P307082	NM_013904
33	Nrn1	Neuritin 1	2.4	A_55_P2822982	NM_153529
34	Hist2h3c2	Histone cluster 2, H3c2	2.38	A_55_P2142251	BC015270
35	AW551984	Expressed sequence AW551984	2.36	A_55_P2484406	NM_001199556
36	Tmem163	Transmembrane protein 163	2.31	A_52_P30328	NM_028135
37	Mcpt4	Mast cell protease 4	2.31	A_51_P145132	NM_010779
38	Ddc	Dopa decarboxylase	2.29	A_55_P2500104	NM_001190448
39	Cpa3	Carboxypeptidase A3, mast cell	2.24	A_51_P214127	NM_007753
40	Tpm2	Tropomyosin 2, beta	2.21	A_51_P357013	NM_009416
41	Myl4	Myosin, light polypeptide 4	2.18	A_55_P2107045	NM_010858
42	Gm30873	Predicted gene, 30873	2.14	A_66_P108009	AK035526
43	Tceal7	Transcription elongation factor A (SII)-like 7	2.14	A_55_P2012011	NM_001127169
44	Msi2	Musashi RNA-binding protein 2	2.13	A_55_P1992045	NM_054043
45	Frem2	Fras1-related extracellular matrix protein 2	2.1	A_52_P5491	NM_172862
46	Cacna1g	Calcium channel, voltage-dependent, T type, alpha 1G subunit	2.1	A_51_P466910	NM_009783
47	Lpar3	Lysophosphatidic acid receptor 3	2.09	A_51_P134452	NM_022983
48	Cks1b	CDC28 protein kinase 1b	2.09	A_66_P137121	NM_016904
49			2.05	A_30_P01028956	chr1:193815525-193825775_F
50	Ddc	Dopa decarboxylase	2.04	A_52_P63905	NM_016672
51	Birc5	Baculoviral IAP repeat-containing 5	2.04	A_55_P1983768	NM_009689
52			2.02	A_55_P2024799	ENSMUST00000120032

Table 4. Twenty gene probes at 0 days of age were significantly downregulated in the pooled ventricular tissues of *TNNT2*$^{\Delta K210/\Delta K210}$ mice.

Downregulated at birth					
	Gene_Symbol	Gene name	Fold change	Probe ID	Genbank accession
1	Spp1	Secreted phosphoprotein 1	−9.64	A_51_P358765	NM_009263
2	Wfdc18	WAP four-disulfide core domain 18	−4.10	A_55_P2483194	NM_007969
3			−3.58	A_55_P2732888	AK081140
4	Rab7b	RAB7B, member RAS oncogene family	−3.51	A_52_P244682	NM_145509
5	Arl8a	ADP-ribosylation factor-like 8A	−3.35	A_51_P224593	NM_026823
6			−3.07	A_30_P01023385	chr15:38639259-38639546_R
7	Iqsec3	IQ motif and Sec7 domain 3	−2.93	A_55_P2067221	NR_110358
8	Pcf11	Cleavage and polyadenylation factor subunit homolog (*S. cerevisiae*)	−2.88	A_55_P2916983	NM_029078
9	LOC433461	Uncharacterized LOC433461	−2.81	A_55_P2258612	AK051942
10			−2.61	A_30_P01020550	chr13:28490070-28492645_R
11			−2.57	A_55_P2730621	AK041267
12	Ube2t	Ubiquitin-conjugating enzyme E2T (putative)	−2.51	A_55_P2719130	ENSMUST00000139617
13	Aqp8	Aquaporin 8	−2.46	A_55_P2318584	NM_007474
14			−2.45	A_55_P2387284	BC099970
15	Tex19.2	Testis expressed gene 19.2	−2.42	A_51_P503736	NM_027622
16			−2.26	A_55_P1971614	ENSMUST00000120168
17	Nudt3	Nudix (nucleotide diphosphate linked moiety X)-type motif 3	−2.17	A_55_P2091691	NM_019837
18			−2.15	A_55_P2129219	NAP113071-1
19	Siglech	Sialic acid binding Ig-like lectin H	−2.12	A_55_P2141013	NM_178706
20	Gnl1	Guanine nucleotide binding protein-like 1	−2.1	A_55_P2177173	NM_008136

Table 5. Thirty gene probes at 1 week of age were significantly downregulated in the pooled ventricular tissues of *TNNT2*$^{\Delta K210/\Delta K210}$ mice.

Downregulated at 1 week					
	Gene_Symbol	Gene name	Fold change	Probe ID	Genbank accession
1	Spp1	Secreted phosphoprotein 1	−10.08	A_51_P358765	NM_009263
2	Ranbp2	RAN binding protein 2	−5.08	A_55_P2730481	AK040322
3	Ppp1r12b	Protein phosphatase 1, regulatory (inhibitor) subunit 12B	−3.85	A_55_P2340221	ENSMUST00000141419
4	Brd4	Bromodomain containing 4	−3.69	A_55_P2174022	NM_198094
5	Acta2	Actin, alpha 2, smooth muscle, aorta	−3.63	A_52_P644232	AK033744
6			−3.12	A_55_P1998987	NAP104240-1
7			−3.00	A_66_P109246	CA584427
8	Rab7b	RAB7B, member RAS oncogene family	−2.95	A_52_P244682	NM_145509
9	Ubxn10	UBX domain protein 10	−2.90	A_55_P2797826	NM_001285928
10			−2.75	A_65_P01058	BM934532
11			−2.60	A_30_P01032942	chr4:94742359-94822969_F
12	6430519N07Rik	RIKEN cDNA 6430519N07 gene	−2.59	A_55_P2205226	AK032319
13	Zranb2	Zinc finger, RAN-binding domain containing 2	−2.57	A_55_P2814946	ENSMUST00000152882
14	Npas4	Neuronal PAS domain protein 4	−2.56	A_55_P1975215	NM_153553
15	Ptch2	Patched homolog 2	−2.52	A_55_P1999408	ENSMUST00000030443
16	Lad1	Ladinin	−2.52	A_66_P123595	NM_133664
17	Aspg	Asparaginase homolog (*S. cerevisiae*)	−2.44	A_52_P338956	NM_001081169
18			−2.38	A_30_P01024823	chrX:34360500-34388500_F
19			−2.37	A_66_P122719	AK081938
20	Ccdc15	Coiled-coil domain containing 15	−2.37	A_51_P147651	NM_001081429
21			−2.36	A_55_P2782833	AW495160
22	Fos	FBJ osteosarcoma oncogene	−2.35	A_55_P2910184	NM_010234
23	Fam118a	Family with sequence similarity 118, member A	−2.33	A_55_P2147886	AK082151
24			−2.19	A_55_P2730621	AK041267
25	ND4	NADH dehydrogenase subunit 4	−2.16	A_51_P245525	AK144853
26	Lrtm1	Leucine-rich repeats and transmembrane domains 1	−2.15	A_51_P326685	NM_176920
27	Phtf1	Putative homeodomain transcription factor 1	−2.11	A_55_P2049448	NM_013629
28			−2.08	A_30_P01023020	chr18:3003075-3016150_R
29	Ivns1abp	Influenza virus NS1A binding protein	−2.04	A_52_P163849	NM_001039511
30	Ceacam2	Carcinoembryonic antigen-related cell adhesion molecule 2	−2.04	A_55_P2386236	NM_001113368

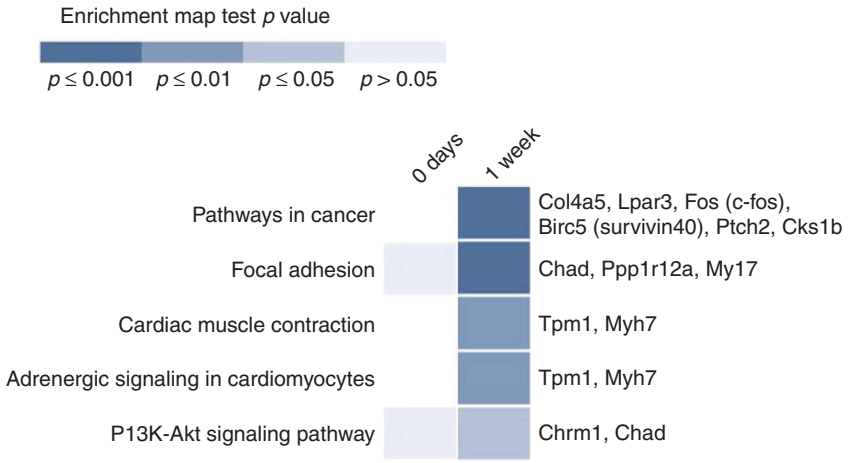

Fig. 3 KEGG enrichment analysis of differentially expressed genes in WT and *TNNT2*$^{\Delta K210/\Delta K210}$ mice at 0 days and 1 week of age. Vertical axis indicates the pathway name. On the right, the genes with significantly altered expression related to these pathways are listed.

cardiac troponin I. The phosphorylation levels of cardiac troponin I were not significantly different between *TNNT2*$^{\Delta K210/\Delta K210}$ mice and wild-type mice at 1 week of age (Fig. 4b, c).

DISCUSSION

The present study showed that the mean ventricular mass and LV end-diastolic dimension and volume of *TNNT2*$^{\Delta K210/\Delta K210}$ mice has already increased at birth and that these mice rapidly develop cardiac dysfunction within 1 week after birth, suggesting that *TNNT2*$^{\Delta K210/\Delta K210}$ mice could be an excellent animal model to investigate the molecular mechanisms of neonatal DCM, especially as this genetic mutation is also found in human DCM. After demonstrating this model's usefulness, we used it to explore the mechanisms of early progression in neonatal DCM.

DNA microarray analyses revealed that the gene expression profiles of *TNNT2*$^{\Delta K210/\Delta K210}$ mice at birth (0 days old) were slightly different from those of wild-type mice and that these differences were even larger 1 week after birth. The expression levels of ANF mRNA, a biomarker of cardiac stress and dysfunction, were not different among the three groups at birth but were significantly increased in *TNNT2*$^{\Delta K210/\Delta K210}$ mice at 1 week of age. Consistent with the result, echocardiographic data also indicated in impaired cardiac function in *TNNT2*$^{\Delta K210/\Delta K210}$ mice at the first week of life, but not at birth, as shown in Fig. 2f. Therefore, we assume that the week following birth is a critical period for the initiation of DCM progression of *TNNT2*$^{\Delta K210/\Delta K210}$ mice, and we are keenly interested in the genes whose expression levels changed during the first week of life (see Tables 3 and 5). KEGG PATHWAY analysis revealed that these genes are involved in five important pathways that might be associated with the pathogenesis and development of DCM. Although the finding of cancer and focal adhesion pathways is of particular interest, we do not have a definite answer how these pathways play a role in neonatal DCM. However, several previous studies have also demonstrated that cancer[13,14] or focal adhesion pathways[15] would be involved in DCM. Six of the genes are involved in cancer-related pathways: four genes (Col4a5, Lpar3, Birc5 (survivin40), and Cks1b) were significantly increased and two genes (Fos and Ptch2) were significantly decreased in *TNNT2*$^{\Delta K210/\Delta K210}$ mice at age 1 week. Huang et al. have suggested that Fos is likewise significantly downregulated in human DCM samples and that it plays an important role in the progression of heart failure as a hub gene for signaling pathways,[16] which is consistent with the present results. On the other hand, Windak et al. have demonstrated that Fos is dispensable for adaptive cardiac hypertrophy using pressure overload-induced cardiac hypertrophy in mice and targeted deletion of Fos in cardiomyocytes.[17] These data indicate that downregulation of Fos is involved in a pathological pathway leading to the development of heart failure but not in a physiological pathway leading to hypertrophy.

Birc5, also known as survivin, inhibits apoptosis and is highly expressed in common human cancers. Birc5 is a critical factor in determining the total number and proliferation of cardiomyocytes and is indispensable for postnatal cardiac development.[18] Although the expression levels of Birc5 decrease with postnatal cardiac development,[19] Birc5 is upregulated in the peri-infarct zone and remote myocardium in human myocardial infarction[20] and elevated in human[18] and rat heart failure,[21] which is consistent with the present findings. Thus the role of Birc5 in the early progression of neonatal DCM is worth further investigation.

The role of the other four cancer-related-pathway genes in the development of cardiomyopathy has not yet been investigated in detail. The COL4A5 gene, which codes non-fibrillar collagen, was reportedly increased in 23 human LV tissue samples from DCM patients.[22] That report, however, is the only one to date that suggests that the upregulation of COL4A5 mRNA may be associated with the fibrotic process in DCM. In the present study, the expression levels of COL4A5 mRNA were increased up to 3.7-fold in *TNNT2*$^{\Delta K210/\Delta K210}$ mice at 1 week of age; it was therefore among the top three most upregulated genes in this study. Although we did not find fibrosis in *TNNT2*$^{\Delta K210/\Delta K210}$ mice at 1 week of age, we have previously shown the progression of fibrosis in *TNNT2*$^{\Delta K210/\Delta K210}$ mice at 8 weeks of age.[10] The upregulation of COL4A5 mRNA may proceed the fibrotic changes. Further investigation is needed to qualify this assumption. Another gene whose expression level changed during the first week of life in *TNNT2*$^{\Delta K210/\Delta K210}$ mice was Lpar3, an embryonic isoform of lysophospholipid G protein-coupled receptor via which small signaling lipids regulate diverse physiological and pathological processes.[23] The upregulation of Lpar3 (2.1 fold) in *TNNT2*$^{\Delta K210/\Delta K210}$ mice may reflect the activation of a fetal gene program.

Although SR dysfunction is known to be one of the earliest insults in heart failure, the expression levels of key molecules

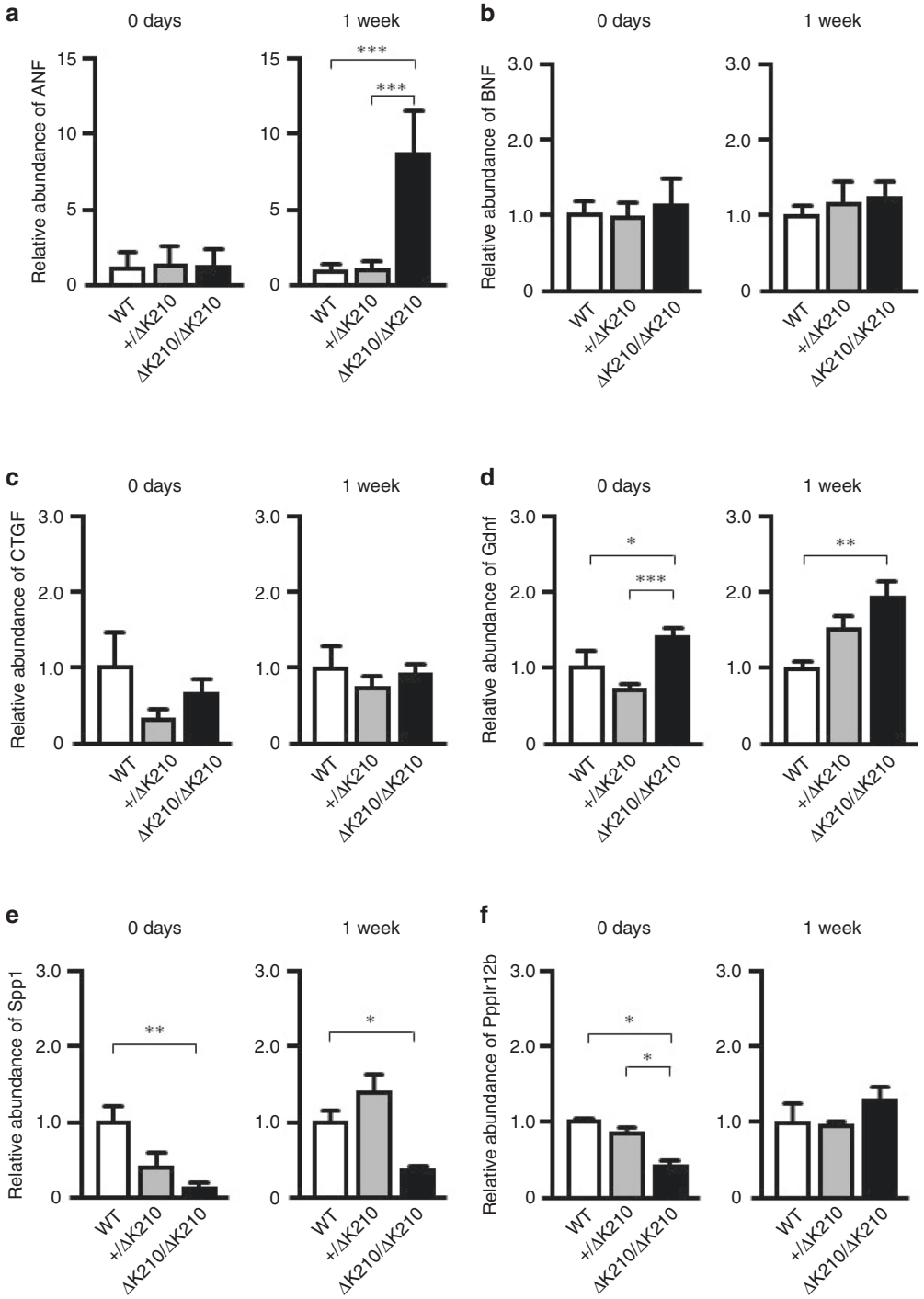

Fig. 4 Verification of the expression patterns through DNA microarray analysis. Quantification of RT-PCR products for **a** ANF ($n > 6$ per group), **b** BNF ($n > 6$ per group), **c** CTGF ($n > 4$ per group), **d** Gdnf ($n > 3$ per group), **e** Spp1 ($n > 3$ per group), and **f** Ppp1r12b ($n > 3$ per group) in ventricular tissues from wild-type (WT), *TNNT2*$^{+/\Delta K210}$, and *TNNT2*$^{\Delta K210/\Delta K210}$ mice at 0 days and 1 week of age. Data are shown as mean ± SEM. *$p < 0.05$, **$p < 0.01$, ***$p < 0.001$ by ANOVA followed by post hoc Tukey's multiple comparison test.

affecting the cardiac SR, including PLN, SERCA2a, and RyR2, remained unchanged in the first week of life. In our previous unpublished examinations, the expression of SERCA2a mRNA was decreased after 4 weeks of age in *TNNT2*$^{\Delta K210/\Delta K210}$ mice. SLN and CSQ1, in contrast, were significantly upregulated within 1 week after birth in *TNNT2*$^{\Delta K210/\Delta K210}$ mice. Interestingly, SLN and CSQ1 are not usually expressed in the ventricles. Rather, SLN is highly expressed in the atrium and skeletal muscles, although the induction of SLN in the ventricles is known to happen under specific conditions.[24,25] CSQ1 is a skeletal type of calsequestrin isoform and the induction of CSQ1 in the ventricles has not been reported. Although we do not know the mechanism by which

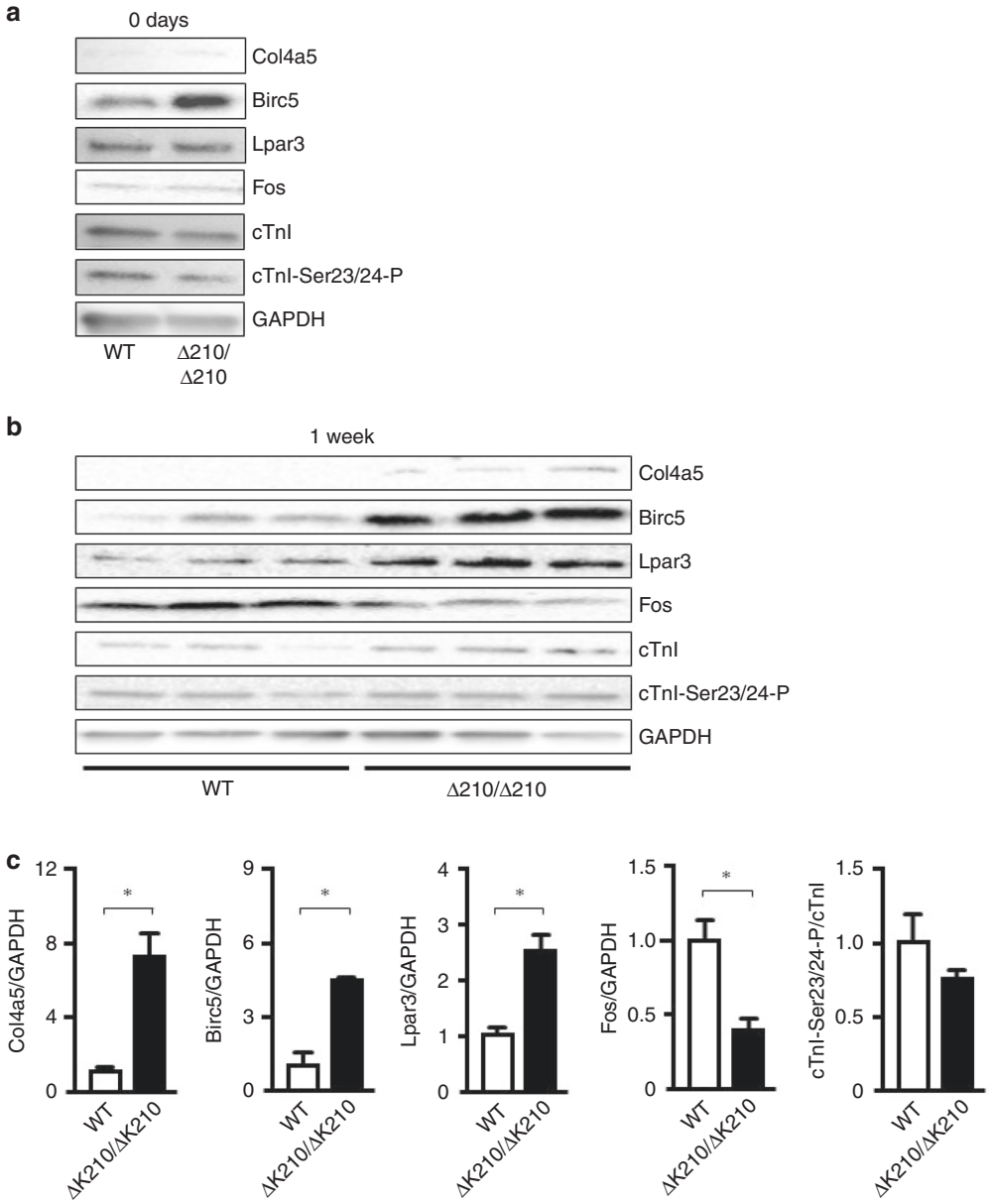

Fig. 5 Western blot analysis verified the expression patterns of DNA microarray analysis. Protein expression levels of Col4a5, Birc5, Lpar3, cTnI, and pcTnI in **a** pooled left ventricular tissues from wild-type and *TNNT2*$^{\Delta K210/\Delta K210}$ mice at 0 days and **b** left ventricular tissues from wild-type and *TNNT2*$^{\Delta K210/\Delta K210}$ mice at 1 week of age. **c** Quantification of protein expression levels of Col4a5, Birc5, and Lpar3 and relative phosphorylation levels of cTnI in wild-type and *TNNT2*$^{\Delta K210/\Delta K210}$ mice at 1 week of age. Data are shown as mean ± SEM. *$p < 0.05$ by ANOVA followed by post hoc Tukey's multiple comparison test.

these skeletal muscle types of SR genes are induced in the neonatal period in *TNNT2*$^{\Delta K210/\Delta K210}$ mice, an epigenetic program might be involved in this phenomenon. Since SLN is a negative regulator of SERCA2a and SERCA1, and since CSQ1 inhibits RyR1 at a physiological luminal calcium concentration,[26] we assume that the upregulation of SLN and CSQ1 may inhibit calcium cycling in the hearts of *TNNT2*$^{\Delta K210/\Delta K210}$ mice, which would play a role in the early progression of cardiac dysfunction in *TNNT2*$^{\Delta K210/\Delta K210}$ mice at 1 week of age.

Because cardiac troponin T isoforms are known to switch from the fetal type (TnT A) to the adult type (TnT E) during the neonatal period,[27,28] and because their Ca^{2+} sensitivities differ with regard to myofibrillar force development,[29,30] we had hypothesized that the timing of the isoform switch might affect the onset of cardiac dysfunction in *TNNT2*$^{\Delta K210/\Delta K210}$ mice. However, we did not find any differences among the three groups in the expression levels of troponin T isoforms, other troponin-related genes, or phosphorylation levels of cardiac troponin I. This finding indicates that the composition of troponin T and associated thin-filament genes is not affected in the progression of cardiac dysfunction.

In conclusion, the mean ventricular mass was already increased at birth in *TNNT2*$^{\Delta K210/\Delta K210}$ mice, and their cardiac function became impaired at age 1 week. Our KEGG PATHWAY analysis revealed that several important pathways such as cancer and focal adhesion might be associated with the pathogenesis and development of neonatal DCM. The present study indicated that *TNNT2*$^{\Delta K210/\Delta K210}$ mice should be an excellent animal model to identify early progression factors of DCM.

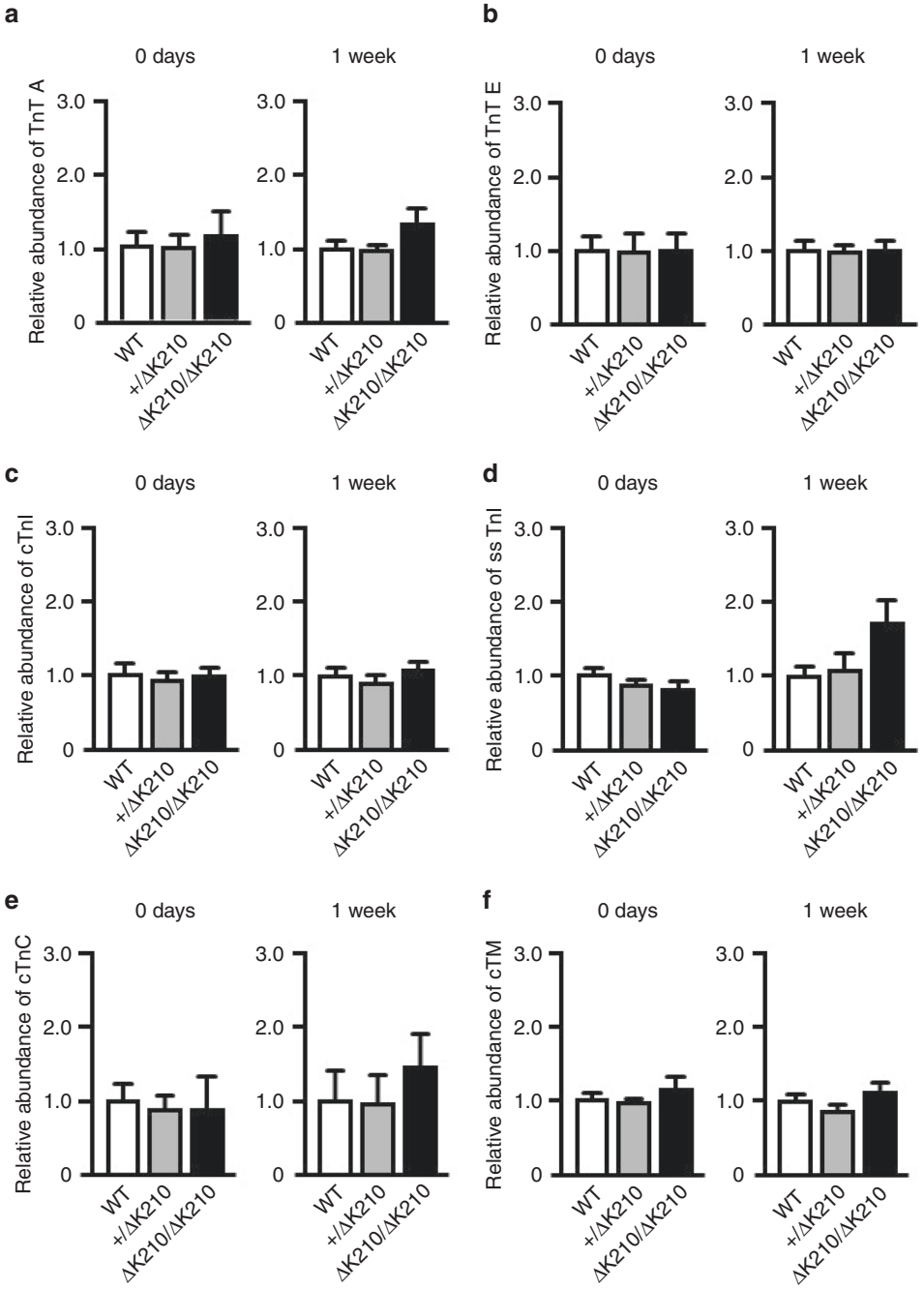

Fig. 6 The expression patterns of troponin-related genes. Quantification of RT-PCR products for **a** TnT A, **b** TnT E, **c** cTnI, **d** ssTnI, **e** cTnC, and **f** cTM in ventricular tissues from wild-type (WT), *TNNT2*$^{+/\Delta K210}$, and *TNNT2*$^{\Delta K210/\Delta K210}$ mice at 0 days and 1 week of age ($n > 7$ per group). Data are shown as mean ± SEM.

ACKNOWLEDGEMENTS

The authors acknowledge Ms. Naoko Tomizawa for her technical support of this research. This work was supported by grants from the Ministry of Education, Culture, Sports, Science and Technology of Japan (to J.T., S. Morimoto, S. Minamisawa), the Vehicle Racing Commemorative Foundation (S. Minamisawa), the Uehara Memorial Foundation (S. Minamisawa), the Descente and Ishimoto Memorial Foundation for Promotion of Sports Science (J.T.), The Jikei University Graduate Student Research Grant (Y.F., S.B.), and the Miyata Cardiology Research Promotion Foundation (S. Minamisawa).

AUTHOR CONTRIBUTIONS

J.T., T.F., S.B., and Y.F. conceived and performed the experiments. J.T., S. Morimoto, and S. Minamisawa conducted and supervised the experiments. S. Morimoto and S. Minamisawa designed the experiments. J.T. and S. Minamisawa wrote the manuscript, and all authors discussed the results and commented on the manuscript.

ADDITIONAL INFORMATION

The online version of this article (https://doi.org/10.1038/s41390-020-1016-1) contains supplementary material, which is available to authorized users.

Competing interests: The authors declare no competing interests.

Publisher's note Springer Nature remains neutral with regard to jurisdictional claims in published maps and institutional affiliations.

REFERENCES

1. Lipshultz, S. E. et al. The incidence of pediatric cardiomyopathy in two regions of the United States. *N. Engl. J. Med.* **348**, 1647–1655 (2003).
2. Towbin, J. A. et al. Incidence, causes, and outcomes of dilated cardiomyopathy in children. *JAMA* **296**, 1867–1876 (2006).
3. Daubeney, P. E. et al. Clinical features and outcomes of childhood dilated cardiomyopathy: results from a national population-based study. *Circulation* **114**, 2671–2678 (2006).
4. Lee, T. M. et al. Pediatric cardiomyopathies. *Circ. Res.* **121**, 855–873 (2017).
5. Patel, M. D. et al. Pediatric and adult dilated cardiomyopathy represent distinct pathological entities. *JCI Insight* **2**, e94382 (2017).
6. Tatman, P. D. et al. Pediatric dilated cardiomyopathy hearts display a unique gene expression profile. *JCI Insight* **2**, e94249 (2017).
7. Hanson, E. L. et al. Cardiac troponin T lysine 210 deletion in a family with dilated cardiomyopathy. *J. Card. Fail.* **8**, 28–32 (2002).
8. Martins, E. et al. Familial dilated cardiomyopathy with troponin T K210del mutation. *Rev. Port. Cardiol.* **25**, 295–300 (2006).
9. Mogensen, J. et al. Severe disease expression of cardiac troponin C and T mutations in patients with idiopathic dilated cardiomyopathy. *J. Am. Coll. Cardiol.* **44**, 2033–2040 (2004).
10. Du, C. K. et al. Knock-in mouse model of dilated cardiomyopathy caused by troponin mutation. *Circ. Res.* **101**, 185–194 (2007).
11. Kusakari, Y. et al. Impairment of excitation-contraction coupling in right ventricular hypertrophied muscle with fibrosis induced by pulmonary artery banding. *PLoS ONE* **12**, e0169564 (2017).
12. Kanehisa, M. et al. From genomics to chemical genomics: new developments in KEGG. *Nucleic Acids Res* **34**, D354–D357 (2006).
13. Chen, S. N. et al. DNA damage response/TP53 pathway is activated and contributes to the pathogenesis of dilated cardiomyopathy associated with LMNA (Lamin A/C) mutations. *Circ. Res.* **124**, 856–873 (2019).
14. Hou, N. et al. Activation of Yap1/Taz signaling in ischemic heart disease and dilated cardiomyopathy. *Exp. Mol. Pathol.* **103**, 267–275 (2017).
15. Xiao, J., Li, F., Yang, Q., Zeng, X. F. & Ke, Z. P. Co-expresssion analysis provides important module and pathways of human dilated cardiomyopathy. *J. Cell. Physiol.* **235**, 494–503 (2020).
16. Huang, H. et al. Identification of potential gene interactions in heart failure caused by idiopathic dilated cardiomyopathy. *Med. Sci. Monit.* **24**, 7697–7709 (2018).
17. Windak, R. et al. The AP-1 transcription factor c-Jun prevents stress-imposed maladaptive remodeling of the heart. *PLoS ONE* **8**, e73294 (2013).
18. Levkau, B. et al. Survivin determines cardiac function by controlling total cardiomyocyte number. *Circulation* **117**, 1583–1593 (2008).
19. Sheng, L. et al. Downregulation of Survivin contributes to cell-cycle arrest during postnatal cardiac development in a severe spinal muscular atrophy mouse model. *Hum. Mol. Genet.* **27**, 486–498 (2018).
20. Santini, D. et al. Surviving acute myocardial infarction: survivin expression in viable cardiomyocytes after infarction. *J. Clin. Pathol.* **57**, 1321–1324 (2004).
21. Abbate, A. et al. Myocardial expression of survivin, an apoptosis inhibitor, in aging and heart failure. An experimental study in the spontaneously hypertensive rat. *Int. J. Cardiol.* **111**, 371–376 (2006).
22. Gil-Cayuela, C. et al. New altered non-fibrillar collagens in human dilated cardiomyopathy: role in the remodeling process. *PLoS ONE* **11**, e0168130 (2016).
23. Wang, F. et al. Developmental changes in lysophospholipid receptor expression in rodent heart from near-term fetus to adult. *Mol. Biol. Rep.* **39**, 9075–9084 (2012).
24. Pashmforoush, M. et al. Nkx2-5 pathways and congenital heart disease; loss of ventricular myocyte lineage specification leads to progressive cardiomyopathy and complete heart block. *Cell* **117**, 373–386 (2004).
25. Voit, A. et al. Reducing sarcolipin expression mitigates Duchenne muscular dystrophy and associated cardiomyopathy in mice. *Nat. Commun.* **8**, 1068 (2017).
26. Beard, N. A., Sakowska, M. M., Dulhunty, A. F. & Laver, D. R. Calsequestrin is an inhibitor of skeletal muscle ryanodine receptor calcium release channels. *Biophys. J.* **82**, 310–320 (2002).
27. Wang, Q., Reiter, R. S., Huang, Q. Q., Jin, J. P. & Lin, J. J. Comparative studies on the expression patterns of three troponin T genes during mouse development. *Anat. Rec.* **263**, 72–84 (2001).
28. Wei, B. & Jin, J. P. TNNT1, TNNT2, and TNNT3: isoform genes, regulation, and structure-function relationships. *Gene* **582**, 1–13 (2016).
29. Pinto, J. R. et al. Fetal cardiac troponin isoforms rescue the increased Ca2+ sensitivity produced by a novel double deletion in cardiac troponin T linked to restrictive cardiomyopathy: a clinical, genetic, and functional approach. *J. Biol. Chem.* **286**, 20901–20912 (2011).
30. Venkatraman, G., Gomes, A. V., Kerrick, W. G. & Potter, J. D. Characterization of troponin T dilated cardiomyopathy mutations in the fetal troponin isoform. *J. Biol. Chem.* **280**, 17584–17592 (2005).